

Accepted Manuscript

Experimental and theoretical investigation of stable diastereomeric conformations of biscarboline amides in solution

Miao-Miao Liang, Yang-Yang Ma, Liang Zhu, Yun-Jing Jia, Hua-Jie Zhu, Wan Li, Bei-Dou Zhou



PII: S0040-4020(18)30737-3

DOI: [10.1016/j.tet.2018.06.037](https://doi.org/10.1016/j.tet.2018.06.037)

Reference: TET 29633

To appear in: *Tetrahedron*

Received Date: 9 April 2018

Revised Date: 13 June 2018

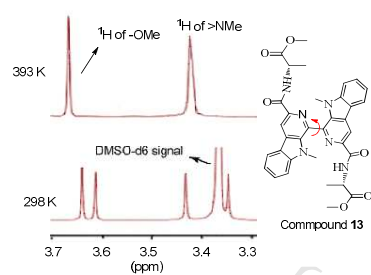
Accepted Date: 15 June 2018

Please cite this article as: Liang M-M, Ma Y-Y, Zhu L, Jia Y-J, Zhu H-J, Li W, Zhou B-D, Experimental and theoretical investigation of stable diastereomeric conformations of biscarboline amides in solution, *Tetrahedron* (2018), doi: 10.1016/j.tet.2018.06.037.

This is a PDF file of an unedited manuscript that has been accepted for publication. As a service to our customers we are providing this early version of the manuscript. The manuscript will undergo copyediting, typesetting, and review of the resulting proof before it is published in its final form. Please note that during the production process errors may be discovered which could affect the content, and all legal disclaimers that apply to the journal pertain.

Experimental and Theoretical Investigation of Stable Diastereomeric Conformations of Biscarboline Amides in Solution

Miao-Miao Liang, Yang-Yang Ma, Liang Zhu, Yun-Jing Jia, Hua-Jie Zhu, Wan Li, Bei-Dou Zhou



Experimental and Theoretical Investigation of Stable Diastereomeric Conformations of Biscarboline Amides in Solution

Miao-Miao Liang^{a,†}, Yang-Yang Ma^{a,†}, Liang Zhu^a, Yun-Jing Jia^a, Hua-Jie Zhu^{a,*},
Wan Li^a, Bei-Dou Zhou^{b,*}

^aCollege of Pharmacy, Chinese Center for Chirality, Hebei University, 071002, China.

^bSchool of Pharmacy and Medical Technology, Putian University, 351100, Putian, Fujian, China

[†] These authors contributed equally to this work

*Correspondence and requests for materials should be addressed to H.-J. Z. (zhuhuajie@hotmail.com, hjzhu2017@163.com) or B.-D. Z. (beidouzhou@ptu.edu.cn)

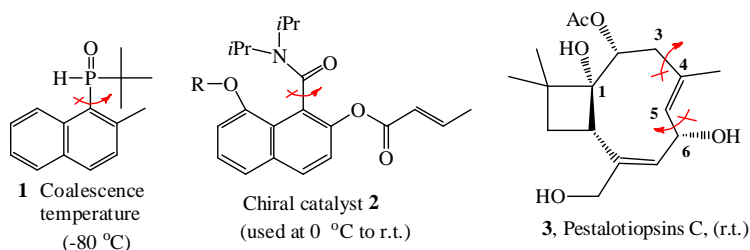
Abstract

Stable axial conformations generally exist only when the single bond's (axis') rotation was sterically hindered in solution. Herein, we firstly show that two stable conformations could be observed in solution by ^1H and ^{13}C NMR experiments when the single bond rotates freely. Its coalescence temperature was measured up to 120 °C when we took compound **13** as an example. The ratio of the two stable conformations was computed using quantum methods. The predicted results matched with the experimental results well. The conversion barrier between two conformers was estimated by potential energy scan (PES) and transition state (TS) calculations at the B3LYP/6-311+G(d) level. Furthermore, its stereochemistry was also well studied by comparing theoretical electronic circular dichroism (ECD) spectra with the experimental one.

Keywords: axial conformations, biscarboline amides, experimental investigation, theoretical investigation

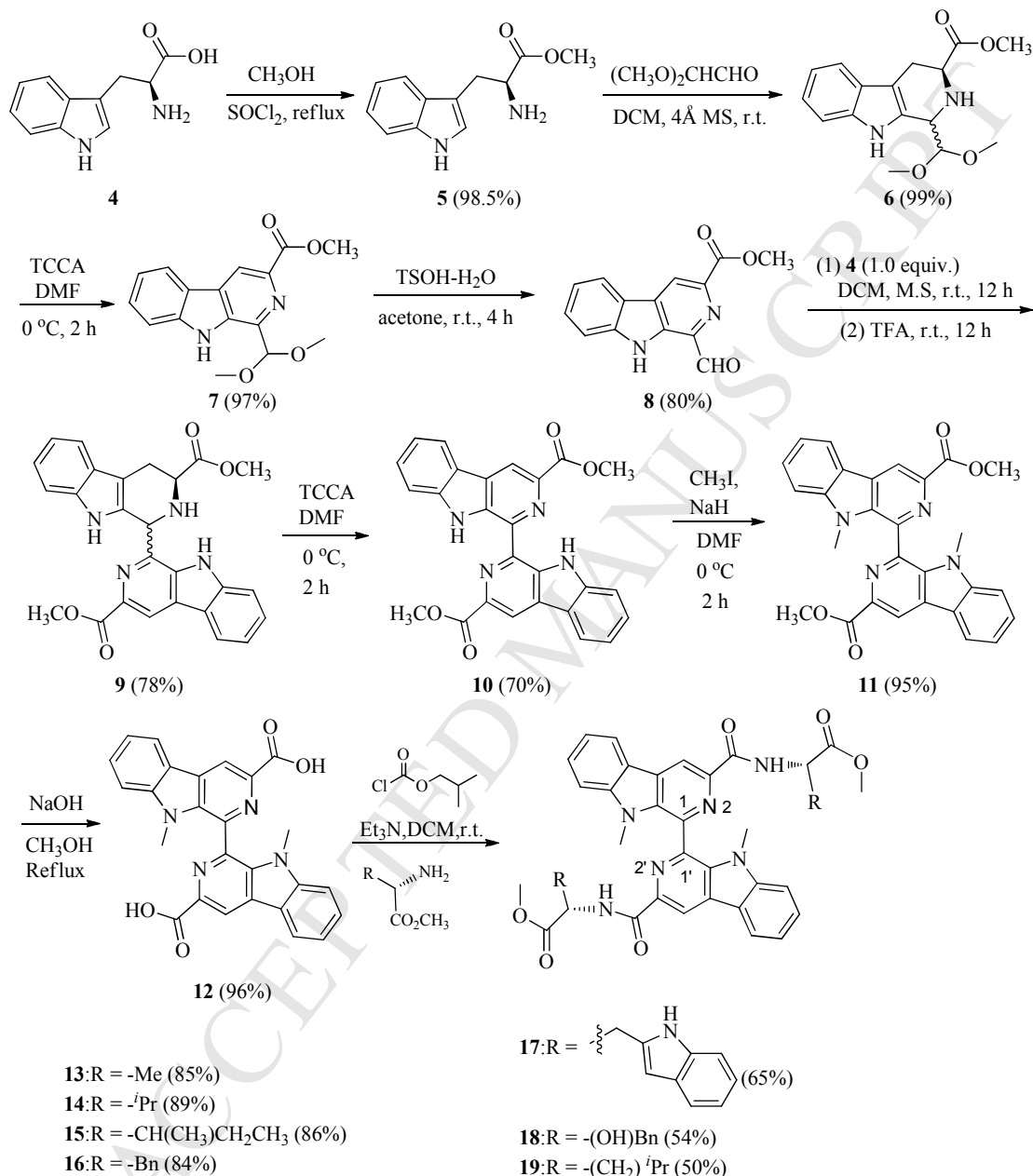
Introduction

Conformational distributions of chiral compounds in solution contribute significantly to their functions like catalysis in enantioselective additions,¹ bioactivities² and the others.³ In terms of bioactivities, atropisomer chirality of anthranilic acid derivatives can lead to distinct entities with specific property. In many cases, it is difficult to record the NMR signals of two different stable conformations in solution since the exchange rate between two conformations is very fast. Many valuable studies reported conformational conversions at very low temperatures, such as $-80\text{ }^{\circ}\text{C}$,⁴ because of the low conversion barriers like 12.4 kcal/mol .^{5,6} It is also difficult to observe the isolated ^1H NMR spectra at room temperature. Taking compound **1** as an example,⁷ in order to record two sets of ^1H NMR clearly, the temperature was cooled as low as $-60\text{ }^{\circ}\text{C}$. If the substituent is bulky enough to block the single bond's rotation, it is possible to isolate the atropisomers and use one of them, such as **2** as a chiral auxiliary in asymmetric reactions.⁸ Caryophyllene C (**3**) was isolated from the fungus of *Trichoderma* sp., which has two sets of ^1H NMR at room temperature with the calculated transition barrier being 19.6 kcal/mol at the B3LYP/6-311+G(d) level in the gas phase at room temperature. This energy barrier could restrict 9-membered ring interconversion.⁹ Indeed, the temperature in NMR spectrometers ranged from 95 K to 450 K . In this study, we report the ^1H NMR study of biscarbolone amides at room temperature in chloroform and the results that the single bond (axis) can rotate freely. Two sets of recorded ^1H and ^{13}C NMR spectra exhibit that there are two stable conformers in chloroform.



Results and Discussion

Synthesis of chiral biscarboline derivatives is illustrated below on the basis of our previous reports.^{10,11} The reaction condition is mild, and the over yield is up to 60% (Scheme 1).



Scheme 1. Synthesis of biscarboline amides **13** to **19**.

Chiral biscarboline amides **13** to **19** may have one set of ¹H and ¹³C NMR spectra theoretically since there is no any atom or group adjacent to the single bond (C1-C1') to sterically hinder its rotation. However, two sets of ¹H and ¹³C NMR spectra were recorded in CDCl₃ at room temperature (Fig. 1). For example, the methyl ¹H NMR signals of -OMe and >NMe displayed two sets of signals. Mostly, other protons also exhibited two sets of signals although some ¹H NMR signals overlapped severely. Majority of carbons had two sets of ¹³C NMR signals too. There were likely two main chiral isomers in solution.

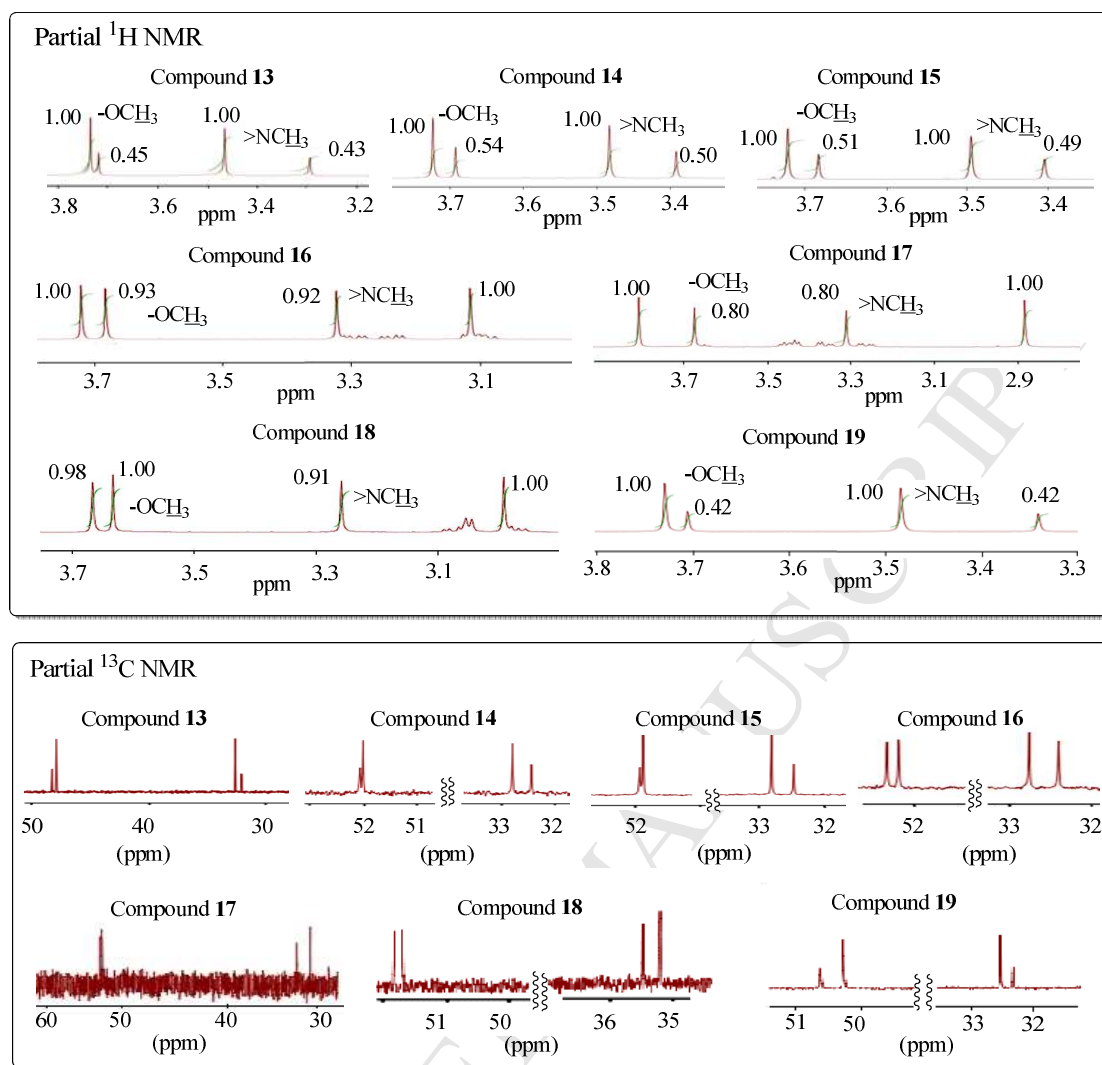


Fig. 1 The recorded partial two sets of ^1H NMR and ^{13}C NMR spectra for $-\text{OMe}$ and $>\text{NMe}$ of **13** to **19**, respectively. The data listed near the proton signals of ^1H NMR spectra are the integration value of this signal. The green lines that cross the proton signals are the integration lines in ^1H NMR spectra

To investigate the phenomena, compound **13** was chosen as a typical example for further study. One HPLC peak of **13** was recorded through chiral columns (Chiralcel series of $-\text{OB-H}$, $-\text{OD-H}$, $-\text{IA}$, $-\text{IB}$, $-\text{IC}$ and $-\text{ID}$) and diethyl pyridine column (see SI for details). Only single peak was recorded. Therefore, it may be only one product existed in solution instead of two stable epimers or two compounds.

Theoretically, the two sets of ^1H and ^{13}C NMR spectra might be caused by partial racemization of the L-alanine ester. To exclude the possibility, racemic L-alanine was used for esterification firstly. The racemic esters then reacted with **12**. Compound **12** had two $-\text{CO}_2\text{H}$ groups which could react with either single L-alanine ester (L-**13**) or D-alanine ester (D-**13**), or the complex of one L-alanine ester and one D-alanine ester (D,L-**13** or L,D-**13**). Thus, it afforded a mixture (M-**13**) of three diastereomeric compounds. Theoretically, the ratio of the three compounds of L-**13**: (D,L)/ (L,D)-**13**:D-**13** should be 1:2:1. Indeed, this was confirmed by HPLC

analysis using Chiracel IC column (Fig. 2). Once L-**13** was added into the racemic sample (M-**13**), the relative area of the third signal increased. This confirmed that the sample **13** obtained in Scheme 1 was an optically pure L-type structure. It showed the reaction condition is quite mild. No partial racemization of **13** happened when the corresponding L-amino acid ester reacted with the intermediate **12** under the reaction conditions we used.

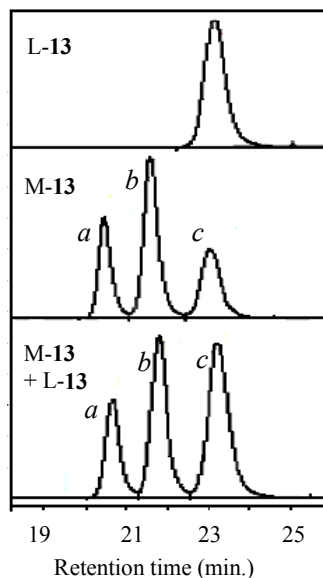


Fig. 2 HPLC analyses for L-**13**, mixture (M-**13**) of products derived from racemic L-alanine ester reacted with **12** and a mixture of M-**13** and L-**13**. The mixture of CH₂Cl₂ and EtOH (v/v=70:30) was used as an eluent by Chiracel IC column. Upper: HPLC signals of the obtained pure product L-**13** in experiment. Only one signal was recorded at a retention time of 23.9 min. Middle: HPLC signals of the mixture (M-**13**) of racemic L-alanine ester reacted with compound **12**. Three signals (*a*, *b*, and *c*) were recorded with a relative area ratio namely 1:2:1. The retention times were 20.8, 21.9 and 23.5 min., respectively. Bottom: HPLC signals of the mixture of M-**13** and L-**13**. The retention times were 20.6, 21.7 and 23.2 min., respectively. The relative area of signal *c* increased when L-**13** was added.

As a typical characteristic of the two stable conformations in solution, the temperature (coalescence temperature) can be raised to “fuse” the two sets of NMR into one. Solvent was replaced then by DMSO-d₆ since it needed a high temperature to “fuse” them. When the temperature was 50 °C, the ¹H NMR signals of –OMe contained two isolated peaks. The two signals gradually became one peak till the measurement temperature raised up to 80 °C (Fig. 3, TMS as an internal standard)(Fig. 3), but the frequency differences between the two conformations decreased from 49.2 Hz at 50 °C to 43.8 Hz at 80 °C, while the frequency differences of protons was 51.6 Hz at room temperature. When the temperature raised to 100°C, the ¹H NMR signal became sharp. However, the proton signals of >NMe were still a bit wide.

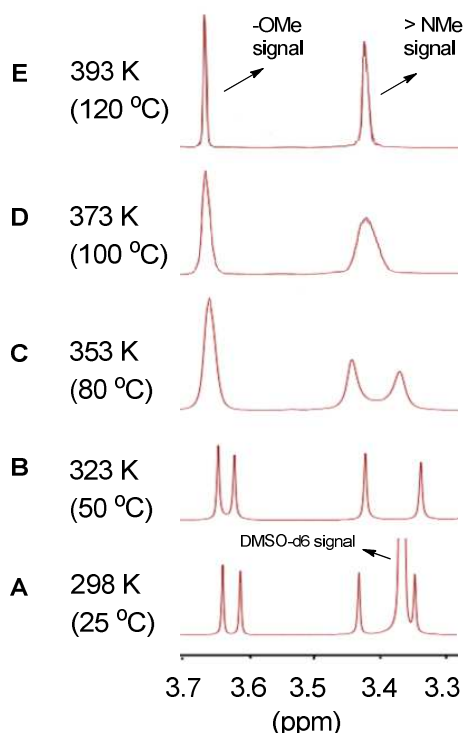


Fig. 3 Chemical shift changes of protons of $-OMe$ when 1H NMR measurement temperature raised from 298 K (25 °C) to 323 K (50 °C), 353 K (80 °C), 373 K (100 °C) and 393 K (120 °C), respectively.

Most reports about conformational studies were carried out at low temperatures as mentioned above,^{3,4} and in those cases low transition state energy like 12.4 kcal/mol could be computed by Eyring equation.^{4,12} In our case, the coalescence temperature was as high as about 80 °C. The computed transition barrier in free energy (ΔG^\ddagger) was 18.4 kcal/mol when the frequency difference of $-OMe$ protons changed from 16.2 Hz (room temperature) to 0 Hz (80 °C) in DMSO- d_6 . Eyring equation is listed as following:

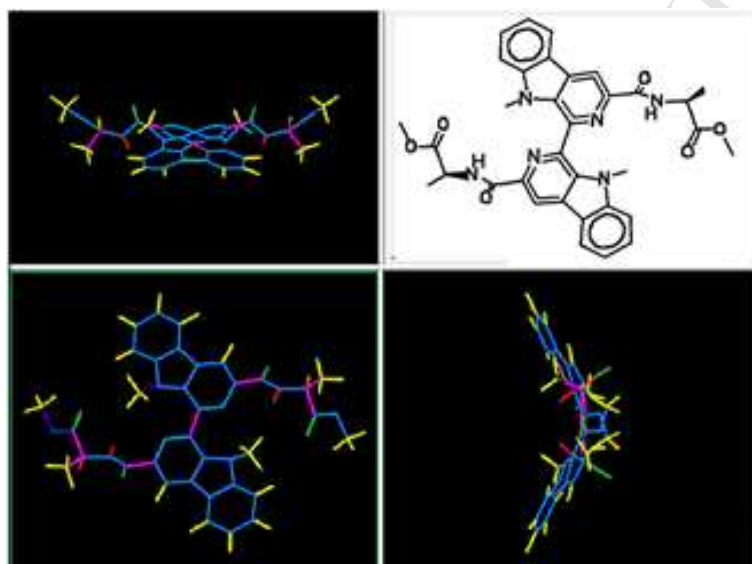
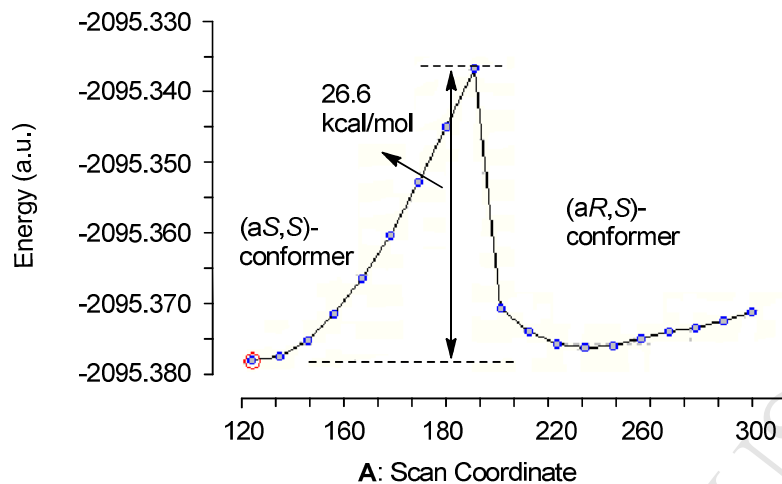
$$\Delta G^\ddagger = RT_c (\ln T_c - \ln k_c + 23.76)$$

Where T_c is the coalescence temperature (K), $k_c = \pi\Delta\nu/2^{-1/2}$, $\Delta\nu$ is difference in the chemical shift of the $-OMe$ protons between two conformations.

However, the protons of $>NCH_3$ also exhibited two signals when the temperature was 353 K (80 °C) (Fig. 3C). Further 1H NMR experiments were performed at higher temperatures, like 373 K and 393 K. The results are illustrated in Figure 3D and 3E. It showed that the sharp signal of $>NCH_3$ was recorded at 393 K. It exhibited that the TS barrier was about 20.6 kcal/mol at 393 K.

To our best knowledge, both two stable conformations observed at very low temperatures are caused by single bond's (axis') rotation restriction. However, in our case, the rotation resistance is not caused by atom(s) or group(s) near the axis. It is necessary and important to investigate this case carefully. Therefore, conformational searches were performed by using MMFF94S force field via two different packages.¹³ All the conformations were optimized at the B3LYP/6-31G(d) level in the gas phase. The optimized conformers with energy within 0-2.5 kcal/mol were selected for re-optimization at the B3LYP/6-311+G(d) level in the gas phase. The geometry with the lowest

energy was selected for potential energy scan (PES) and transition state (TS) calculations, respectively.¹⁴ PES was performed firstly via rotation around C1-C1' at the B3LYP/6-311+G(d) level.¹⁵ The energy reached up to 26.6 kcal/mol via overcoming the conversion barrier from (a*S,S*) to (a*R,S*). The PES curve is illustrated in Fig. 4A. This estimation of rotation resistance around C1-C1' is higher than the free energy barrier (20.6 kcal/mol) using Eyring equation.



B: Orthographic TS views

Fig. 4 (A) The PES scan curve via C1-C1' rotation using B3LYP/6-311+G(d) method. (B) The orthographic TS views obtained at the B3LYP/6-311+G(d) level using the lowest energy conformation as an initial TS structure in computations, and the up-right is its planar TS structure.

Meanwhile, TS barrier energy for conversion from (a*S,S*)-**13** to (a*R,S*)-**13** was calculated at the B3LYP/6-311+G(d) level in the gas phase. The predicted barrier was 24.4 kcal/mol in total electron energy at the B3LYP/6-311+G(d) level. Considering the computed barrier in the gas phase is different from that in liquid by about 0.5-2 kcal/mol using PCM model, or by about 3-6 kcal/mol through adding specific polar solvent in TS structures,¹⁶ we did single point energy computations at the B3LYP/6-311++G(2d,p) level in CHCl₃ using the B3LYP/6-311+G(d)-optimized TS structure and PCM model. This barrier decreased to 23.9 kcal/mol. We then re-computed its barrier at the B3LYP/6-311+G(d,p) level in CHCl₃ using PCM

model, and the geometries were then used for single point energy computations at the B3LYP/6-311++G(2d,p) level in liquid using PCM model. The predicted barrier decreased from 24.4 kcal/mol to 24.0 kcal/mol. The difference of TS barrier between the computed barrier using Eyring equation (based on experimental results) and the predicted barrier using quantum theory was about 4 Kcal/mol. Therefore, the barrier near 20.6 kcal/mol predicted by Eyring equation should be reasonable. The TS structure is illustrated in Fig. 4B. All the TS structures at different basis sets just contained single imaginary frequency or eigenvalue.

In order to explain the ratio of ^1H NMR of L-**13** in CDCl_3 , stable conformations of L-**13** were obtained using MMFF94S force field. After B3LYP/6-31G(d)-optimized geometries were obtained, further accurate geometries were recorded using three methods. Method 1: The optimization was performed at the B3LYP/6-311+G(d) level in the gas phase. Method 2: The optimization was carried out at the B3LYP/6-311++G(2d,p) level in the gas phase. Method 3: The optimization was calculated at the B3LYP/6-311+G(d,p) level in CHCl_3 using PCM model. Different energy data for all geometries are summarized in Table 1. The most stable conformation of (aR,S)-**13** obtained at B3LYP/6-311+G(d) level in the gas phase just occupied about 3%, namely, the ratio of (aS,S)-**13** to (aR,S)-**13** was about 27.8:1. It was also 27.8:1 at the B3LYP/6-311++G(2d,p) level in the gas phase. However, the experimental ratio was 2.22:1 using the methyl protons integration of -OMe, or 2.32:1 using the methyl protons integration of >NMe, or 2.27:1 using their averaged value in experiments. Obviously, both predicted results in the gas phase had big differences from the experimental result. Thus, all the geometries were further optimized at the B3LYP/6-311+G(d,p) level in solution using PCM model. The predicted ratio of (aS,S)-**13** to (aR,S)-**13** turned to be 4.8:1 via the relative energy values analyses. Apparently, the calculated ratio 4.8:1 in solution is close to the experimental result compared to the calculated ratio in gas phase.

Table 1 The conformational structures (from **a** to **h**) for (aS,S)-**13** and (from **a** to **f**) for (aR,S)-**13** obtained at different levels.

Conformer	Method 1 ^a (in the gas phase)		Method 2 ^b (in the gas phase)		Method 3 ^c (in liquid)	
	ΔE ^d	Rel. Fr. ^e	ΔE	Rel. Fr.	ΔE	Rel. Fr.
(aS,S)- a	0.000	1.000	0.000	1.000	0.000	1.000
(aS,S)- b	2.066	0.0304	2.061	0.0306	0.938	0.204
(aS,S)- c	1.743	0.0524	1.567	0.0707	0.981	0.190
(aS,S)- d	4.221	0.0008	4.206	0.00081	1.886	0.0412
(aS,S)- e	3.852	0.0015	3.636	0.0021	1.952	0.0368
(aS,S)- f	3.580	0.0023	3.203	0.0044	2.046	0.0314
(aS,S)- g	3.588	0.0023	3.300	0.0037	2.117	0.0279
(aS,S)- h	4.145	0.0009	4.091	0.00099	- ^f	- ^f
Sum of fractions =		1.091		1.113		1.532
(aR,S)- a	3.386	0.0032	3.368	0.0033	1.092	0.157
(aR,S)- b	2.514	0.0142	2.585	0.0126	-	-
(aR,S)- c	2.456	0.0157	2.336	0.019	1.283	0.114
(aR,S)- d	3.870	0.0014	3.514	0.0026	2.179	0.025

(a <i>R,S</i>)-e	3.862	0.0014	3.652	0.0021	2.256	0.022
(a <i>R,S</i>)-f	3.406	0.0031	-	-	-	-
Sum of fractions =		0.0393		0.0400		0.3192
Ratio of (a <i>S,S</i>):(a <i>R,S</i>)		27.8:1		27.8:1		4.8:1

^a Method 1: optimization at the B3LYP/6-311+G(d) level in the gas phase. ^b Method 2: optimization at the B3LYP/6-311++G(2d,p) level in the gas phase. ^c Method 3: optimization at the B3LYP/6-311+G(d,p) level in CHCl₃ using PCM model. ^d Unit: Kcal/mol for all ΔE data. ^e The relative fraction (Rel. Fr.) means the relative ratio based on their energies. The lowest energy conformation had -2095.3774786 a.u. for (a*S,S*)-**13** using method 1, -2095.4772563 a.u. using method 2, and -2095.444776 a.u. via using method 3. These data were used as the reference zero for relative ratio calculation. ^f The conformation had energy degeneration with others.

The lowest energy geometries (a*S,S*)-**13a** and (a*R,S*)-**13c**, are illustrated in Fig. 5. It is clearly found that the ester moiety (red moiety, Fig. 5, left) of (a*R,S*)-**13c** tended to block the indole moiety rotation (red section, right figure) around the C1-C1' axis. This sterically hindered rotation leads two results. One is the rotation rate is very slow. This is valid for NMR machine determining the shielding constants. The second is leading to the rotation energy barrier increase.

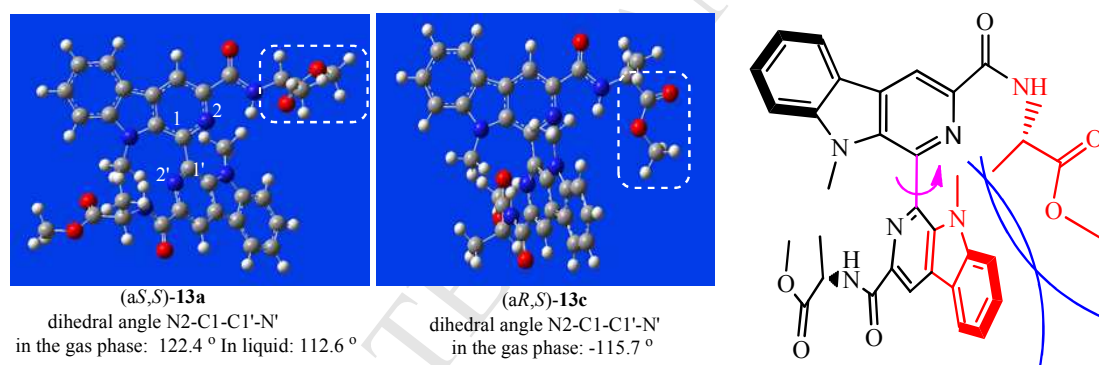


Fig. 5 The most stable conformations of (a*S,S*)-**13a** and (a*R,S*)-**13c**. The big repulsive between the indole moiety and the ester moiety sterically hindered its rotation around C1-C1'.

Electronic circular dichroism (ECD) spectra were also investigated for **13**.^{9,14,16} All the B3LYP/6-311++G(2d,p)-optimized geometries were used for their ECD calculations at the B3LYP/6-311+G(d) level in the gas phase and in liquid, respectively (Fig. 6). Firstly, the simulated ECD spectra for single conformation (a*S,S*)-**13a** (geometry number in Table 1) and single conformation (a*R,S*)-**13c**, which both had the lowest energy in each series of configurations, were compared to each other. They had almost the mirror-image-like curves (Fig. 6A-C). It seemed that the effect of the stereogenic center of amino acid moiety had very small effect on its ECD curve in single conformation even if this stereogenic center was close to the chromophore of >C=O. The ECD curve of single conformation depends on each single conformation's axial chirality (a*S* or a*R*).

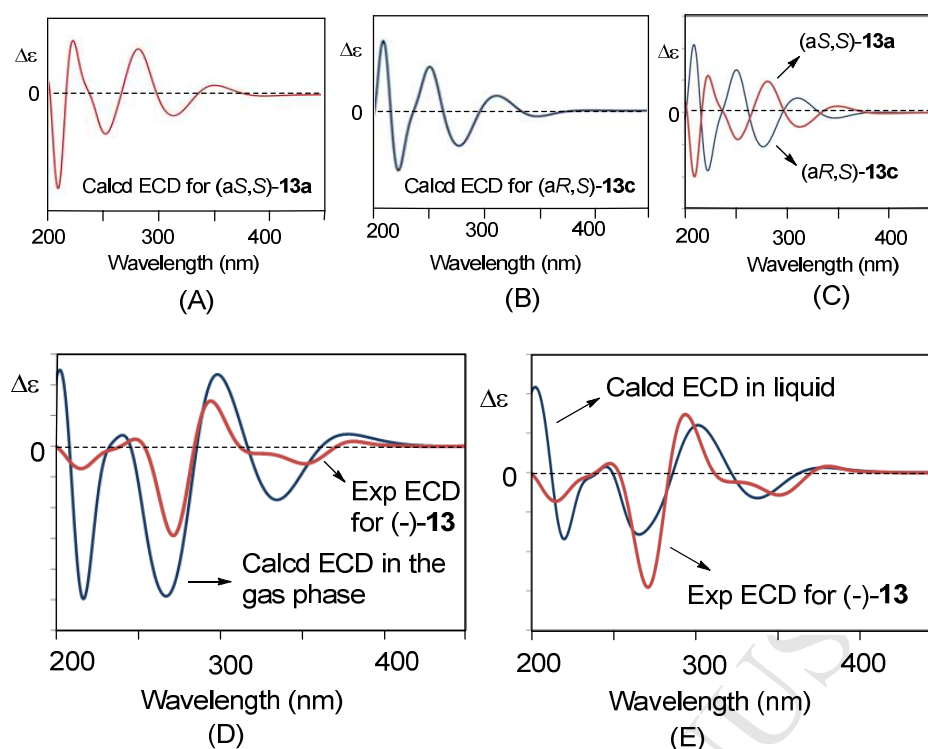


Fig. 6(A) Predicted ECD for single conformation (aS,S)-**13a** with the lowest energy. (B) Predicted ECD for single conformation (aR,S)-**13c** with the lowest energy. (C) Comparison of the ECD spectra between the (aS,S)-**13a** and (aR,S)-**13c**. (D) Comparison of the predicted ECD spectrum using all geometries in the gas phase and the experimental ECD spectrum. (E) Comparison of the predicted ECD spectrum using all geometries in liquid and the experimental ECD spectrum. The standard derivation is 0.25 eV.

Finally, the simulated ECD spectra using all conformations in the gas phase was compared with the experimental ECD spectrum in Fig. 5(D). Then the B3LYP/6-311+G(d)-optimized conformations in CHCl_3 were used in ECD simulations again at the B3LYP/6-311+G(d) level in liquid using PCM model. Both ECD spectra were compared with each other (Fig. 5(E)). The ECD curve predicted that **13** in the gas phase (Fig. 5(D)) has less similarity than the one in liquid (Fig. 5 (E)) when they were compared to the experimental results.

Conclusion

We showed two stable chiral axial conformations of biscarboline amides without single bond's (axis') rotation restriction at room temperature. The results had been confirmed by ^1H and ^{13}C NMR spectra respectively, variable temperature NMR and HPLC analyses taking compound **13** as an example. Furthermore, the conversion TS barrier was obtained. Its ECD was also investigated experimentally and theoretically, and a good agreement between the predicted and experimental ECD spectra was obtained.

Experimental details

General methods

All reactions were monitored by GF_{254} thin layer chromatography (TLC). Flash chromatography was performed using silica gel (200-300 mesh). Optical rotations were performed on an Optical Activity AA-55 polarimeter using a 10 cm cell with a Na 589 nm filter. HPLC

analysis was performed with chiral columns and normal phase chromatographic column. ^1H NMR and ^{13}C NMR were recorded on a Bruker AV-600 spectrometer in CDCl_3 or DMSO-d_6 with tetramethyl-silane (TMS) as a reference. All solvents for the reactions were of reagent grade and were dried and distilled before used.

General procedure for preparation of 13-19

To the solution of **12** (0.45 g, 1 mmol) and Et_3N (0.41 ml, 3.0 mmol) in anhydrous CH_2Cl_2 , isobutyl-chloroformate was added drop-wisely (0.31 ml, 2.4 mmol) at 0°C . Amino acid ester (2.4 mmol) was added after 30 mins. The reaction was warmed to room temperature slowly and detected by TLC until the reaction finished. Then, aqueous HCl solution (1 M) was added to quench the reaction. Aqueous saturated NaHCO_3 solution was used to adjust pH to 7-8 and the mixture was washed with brine, dried over anhydrous Na_2SO_4 . The solution was concentrated under reduced pressure and the residue was purified with silica gel.

Compound **13**: Following the general procedure mentioned above, it was obtained as yellow solid, yield of 85%. MS-ESI, m/z 620.2 $[\text{M}+\text{H}]^+$. $[\alpha]_{\text{D}}^{25}$ -77.52 (c 2.37, CH_2Cl_2). **13A**: ^1H NMR (600 MHz, CDCl_3) δ 9.12 (s, 2H), 8.42 (d, $J = 8.4$ Hz, 1H), 8.33 (t, $J = 7.5$ Hz, 2H), 7.68 (ddd, $J = 11.1, 8.2, 1.0$ Hz, 2H), 7.52 (d, $J = 8.3$ Hz, 1H), 7.44 – 7.40 (m, 2H), 4.94 – 4.88 (m, 2H), 3.73 (s, 4H), 3.46 (s, 5H), 1.47 (d, $J = 7.2$ Hz, 4H). ^{13}C NMR (151 MHz, CDCl_3) δ 173.47, 164.71, 143.16, 138.45, 137.97, 137.36, 131.21, 129.34, 122.05, 121.43, 120.96, 114.94, 110.13, 52.34, 47.97, 32.67, 18.43. **13B**: ^1H NMR (600 MHz, CDCl_3) δ 9.12 (s, 2H), 8.37 (d, $J = 7.7$ Hz, 1H), 8.33 (t, $J = 7.5$ Hz, 2H), 7.68 (ddd, $J = 11.1, 8.2, 1.0$ Hz, 2H), 7.46 (d, $J = 8.3$ Hz, 1H), 7.44 – 7.40 (m, 2H), 4.84 – 4.81 (m, 1H), 3.71 (s, 2H), 3.29 (s, 1H), 1.52 (d, $J = 7.2$ Hz, 2H). ^{13}C NMR (151 MHz, CDCl_3) δ 173.17, 165.00, 142.96, 138.50, 138.23, 137.30, 130.89, 129.30, 122.13, 121.46, 120.96, 115.03, 109.92, 52.38, 48.33, 32.15, 18.29. Elemental analysis for $\text{C}_{34}\text{H}_{32}\text{N}_6\text{O}_6$: calcd. C: 65.80, H: 5.20, N: 13.54, found: C:65.70, H:5.31, N:13.47.

Compound **14**. Yellow solid, yield of 89%. MS-ESI, m/z 676.5 $[\text{M}+\text{H}]^+$. $[\alpha]_{\text{D}}^{25}$ -27.66 (c 2.41, CH_2Cl_2). **14A**: ^1H NMR (600 MHz, CDCl_3) δ 9.12 (s, 1H), 8.49 (d, $J = 9.3$ Hz, 1H), 8.34 (d, $J = 2.9$ Hz, 1H), 7.71 – 7.66 (m, 2H), 7.52 (d, $J = 8.3$ Hz, 1H), 7.45 – 7.41 (m, 2H), 4.82 (dd, $J = 9.3, 5.3$ Hz, 1H), 3.72 (s, 4H), 3.48 (s, 4H), 2.30 – 2.21 (m, 2H), 0.97 (d, $J = 6.8$ Hz, 4H), 0.88 (d, $J = 6.8$ Hz, 4H). ^{13}C NMR (151 MHz, CDCl_3) δ 172.53, 165.17, 143.26, 138.53, 138.02, 137.48, 131.32, 129.31, 121.99, 121.47, 120.92, 114.94, 110.13, 57.46, 52.02, 32.81, 31.48, 19.18, 18.05. **14B**: ^1H NMR (600 MHz, CDCl_3) δ 9.13 (s, 1H), 8.39 (d, $J = 9.1$ Hz, 1H), 8.33 (d, $J = 2.9$ Hz, 1H), 7.71 – 7.66 (m, 2H), 7.47 (d, $J = 8.3$ Hz, 1H), 7.45 – 7.41 (m, 2H), 4.78 (dd, $J = 9.1, 5.6$ Hz, 1H), 3.69 (s, 2H), 3.39 (s, 2H), 2.30 – 2.21 (m, 2H), 1.01 (d, $J = 6.8$ Hz, 2H), 0.91 (d, $J = 6.8$ Hz, 2H). ^{13}C NMR (151 MHz, CDCl_3) δ 172.14, 165.17, 143.09, 138.51, 138.22, 137.44, 131.23, 129.33, 121.12, 121.53, 121.00, 115.08, 109.87, 57.59, 52.08, 32.46, 31.26, 19.27, 18.17. Elemental analysis for $\text{C}_{38}\text{H}_{40}\text{N}_6\text{O}_6$: calcd. C: 67.44, H: 5.96, N: 12.42, found: C:67.28, H:6.11, N:12.36.

Compound **15**. Yellow solid, yield of 86%. MS-ESI, m/z 704.6 $[\text{M}+\text{H}]^+$. $[\alpha]_{\text{D}}^{25}$ -56.80 (c 2.47, CH_2Cl_2). **15A**: ^1H NMR (600 MHz, CDCl_3) δ 9.12 (s, 2H), 8.48 (d, $J = 9.2$ Hz, 1H), 8.34 (d, $J = 3.3$ Hz, 1H), 7.71 – 7.66 (m, 2H), 7.52 (d, $J = 8.3$ Hz, 1H), 7.43 (td, $J = 7.5, 2.4$ Hz, 2H), 4.86 (dd, $J = 9.2, 5.3$ Hz, 1H), 3.72 (s, 4H), 3.49 (s, 4H), 1.99 – 1.94 (m, 1H), 1.50 – 1.40 (m, 2H), 0.92 (d, $J = 6.9$ Hz, 4H), 0.84 (t, $J = 7.4$ Hz, 4H). ^{13}C NMR (151 MHz, CDCl_3) δ 172.50, 165.02, 143.29, 138.55, 138.09, 137.48, 131.36, 129.29, 121.96, 121.49, 120.91, 114.87, 110.12, 56.74, 51.92, 38.02, 32.84, 25.18, 15.64, 11.36. **15B**: ^1H NMR (600 MHz, CDCl_3) δ 9.12 (s, 2H), 8.39 (d, $J = 9.0$

Hz, 1H), 8.33 (d, $J = 3.4$ Hz, 1H), 7.71 – 7.66 (m, 2H), 7.46 (d, $J = 8.3$ Hz, 1H), 7.43 (td, $J = 7.5$, 2.4 Hz, 2H), 4.84 – 4.80 (m, 1H), 3.68 (s, 2H), 3.40 (s, 2H), 2.05 – 2.00 (m, 1H), 1.20 – 1.13 (m, 2H), 0.97 (d, $J = 6.8$ Hz, 2H), 0.88 (t, $J = 7.4$ Hz, 2H). ^{13}C NMR (151 MHz, CDCl_3) δ 172.02, 165.02, 143.12, 138.30, 138.09, 137.45, 131.28, 129.29, 122.10, 121.56, 120.99, 114.97, 109.82, 56.82, 51.98, 37.82, 32.49, 25.35, 15.71, 11.41. Elemental analysis for $\text{C}_{40}\text{H}_{44}\text{N}_6\text{O}_6$: calcd. C: 68.16, H: 6.29, N: 11.92, found: C:68.04, H:6.38, N:11.91

Compound **16**. Yellow solid, yield of 84%. MS-ESI, m/z 772.6 $[\text{M}+\text{H}]^+$. $[\alpha]_{\text{D}}^{25} +48.25$ (c 2.28, CH_2Cl_2). **16A**: ^1H NMR (600 MHz, CDCl_3) δ 9.09 (s, 1H), 8.44 (d, $J = 8.8$ Hz, 1H), 8.34 (dd, $J = 7.8$, 4.6 Hz, 2H), 7.71 (dt, $J = 15.3$, 7.7 Hz, 2H), 7.46 (d, $J = 1.9$ Hz, 1H), 7.41 (d, $J = 8.3$ Hz, 1H), 7.00 (d, $J = 7.4$ Hz, 2H), 6.96 (t, $J = 7.4$ Hz, 1H), 6.75 (t, $J = 7.7$ Hz, 2H), 5.10 (dt, $J = 8.8$, 5.9 Hz, 1H), 3.72 (s, 3H), 3.11 (s, 3H), 3.29 (dd, $J = 14.1$, 5.4 Hz, 1H), 3.09 (dd, $J = 8.0$, 6.2 Hz, 2H). ^{13}C NMR (151 MHz, CDCl_3) δ 172.03, 164.89, 143.20, 138.40, 137.66, 137.18, 136.17, 131.27, 129.19, 129.02, 129.00, 128.24, 128.22, 126.85, 121.89, 121.44, 120.93, 114.63, 110.33, 52.87, 52.19, 37.92, 32.77. **16B**: ^1H NMR (600 MHz, CDCl_3) δ 9.07 (s, 1H), 8.34 (dd, $J = 7.8$, 4.6 Hz, 2H), 8.29 (d, $J = 7.6$ Hz, 1H), 7.71 (dt, $J = 15.3$, 7.7 Hz, 2H), 7.45 (s, 1H), 7.44 (d, $J = 4.2$ Hz, 1H), 7.04 (d, $J = 7.2$ Hz, 2H), 6.89 (t, $J = 7.5$ Hz, 2H), 6.57 (t, $J = 7.4$ Hz, 1H), 5.05 (td, $J = 7.7$, 5.5 Hz, 1H), 3.68 (s, 3H), 3.32 (s, 3H), 3.23 (dd, $J = 13.9$, 5.8 Hz, 1H), 3.09 (dd, $J = 8.0$, 6.2 Hz, 2H). ^{13}C NMR (151 MHz, CDCl_3) δ 171.89, 164.95, 142.95, 138.33, 137.76, 137.18, 135.58, 131.03, 129.27, 129.04, 129.04, 128.40, 128.40, 126.88, 122.10, 121.42, 121.00, 114.79, 109.95, 53.35, 52.34, 37.68, 32.41. Elemental analysis for $\text{C}_{46}\text{H}_{40}\text{N}_6\text{O}_6$: calcd. C: 71.49, H: 5.22, N: 10.87, found: C:71.35, H:5.33, N:10.83.

Compound **17**. Yellow solid, yield of 65% (0.55g). MS-ESI, m/z 851 $[\text{M}+\text{H}]^+$. $[\alpha]_{\text{D}}^{25} -28.35$ (c 3.65, CH_2Cl_2). **17A**: ^1H NMR (600 MHz, CDCl_3) δ 9.10 (s, 1H), 8.58 (d, $J = 8.8$ Hz, 1H), 8.38 (d, $J = 7.9$ Hz, 1H), 8.34 – 8.28 (m, 2H), 7.74 – 7.69 (m, 1H), 7.49 (t, $J = 7.5$ Hz, 1H), 7.38 (d, $J = 8.3$ Hz, 1H), 7.14 (s, 1H), 6.94 (dd, $J = 5.8$, 3.1 Hz, 1H), 6.78 (dd, $J = 17.3$, 8.3 Hz, 2H), 6.71 (d, $J = 1.6$ Hz, 1H), 5.15 (dt, $J = 10.3$, 5.3 Hz, 1H), 3.67 (d, $J = 7.6$ Hz, 3H), 3.45 (dt, $J = 12.3$, 5.9 Hz, 2H), 3.31 (s, 3H), 3.26 (dd, $J = 15.0$, 5.1 Hz, 1H). ^{13}C NMR (150 MHz, CDCl_3) δ 172.42, 165.41, 142.88, 138.41, 137.24, 136.04, 130.59, 129.27, 127.11, 122.58, 122.31, 121.99, 121.41, 121.05, 119.00, 117.99, 114.57, 111.17, 110.31, 109.95, 108.77, 52.39, 52.31, 31.48, 26.87. **17B**: ^1H NMR (600 MHz, CDCl_3) δ 9.07 (s, 1H), 8.55 (d, $J = 7.1$ Hz, 1H), 8.38 (d, $J = 7.9$ Hz, 1H), 8.34 – 8.28 (m, 2H), 7.67 (t, $J = 7.6$ Hz, 1H), 7.43 (t, $J = 7.8$ Hz, 3H), 7.32 (d, $J = 8.3$ Hz, 1H), 7.14 (s, 1H), 6.87 (t, $J = 7.5$ Hz, 1H), 6.74 (dd, $J = 6.0$, 3.0 Hz, 2H), 6.68 (d, $J = 1.7$ Hz, 1H), 5.04 (dd, $J = 12.4$, 5.5 Hz, 1H), 3.81 (s, 3H), 3.45 (dt, $J = 12.3$, 5.9 Hz, 2H), 3.36 (dd, $J = 15.0$, 5.3 Hz, 1H), 2.88 (s, 3H). ^{13}C NMR (150 MHz, CDCl_3) δ 173.06, 164.92, 143.15, 138.44, 137.90, 137.24, 131.20, 129.31, 127.20, 122.11, 121.97, 121.84, 121.36, 120.99, 119.31, 118.34, 114.62, 111.17, 110.90, 109.75, 109.08, 52.56, 52.29, 32.82, 27.57. Elemental analysis for $\text{C}_{46}\text{H}_{40}\text{N}_6\text{O}_8$: calcd. C: 70.57, H: 4.98, N: 13.17, found: C:70.38, H:5.13, N:13.14.

Compound **18**. Yellow solid, yield of 54% (0.43g). MS-ESI, m/z 805 $[\text{M}+\text{H}]^+$. $[\alpha]_{\text{D}}^{25} -5.34$ (c 6.87, CH_2Cl_2). **18A**: ^1H NMR (600 MHz, CDCl_3) δ 8.91 (s, 2H), 8.42 (d, $J = 8.3$ Hz, 1H), 8.12 (t, $J = 7.6$ Hz, 2H), 7.53 (dt, $J = 19.6$, 7.7 Hz, 2H), 7.35 (dd, $J = 8.3$, 4.5 Hz, 2H), 7.27 (dt, $J = 17.1$, 7.5 Hz, 2H), 6.74 (dd, $J = 16.6$, 8.4 Hz, 4H), 6.34 (d, $J = 8.4$ Hz, 2H), 6.27 (d, $J = 8.3$ Hz, 2H), 4.92 (dd, $J = 13.3$, 7.3 Hz, 1H), 3.67 (s, 3H), 3.26 (s, 3H), 3.09 – 3.06 (m, 1H), 3.05 (d, $J = 5.9$ Hz, 2H). ^{13}C NMR (150 MHz, CDCl_3) δ 171.65, 164.19, 153.96, 141.80, 137.33, 136.85, 136.19, 130.02, 129.06, 128.26, 126.31, 120.26, 120.3, 119.94, 114.5, 113.7, 108.9, 52.13, 51.54, 35.37,

31.53. **18B**: ^1H NMR (600 MHz, CDCl_3) δ 8.91 (s, 2H), 8.30 (d, $J = 7.6$ Hz, 1H), 8.12 (t, $J = 7.6$ Hz, 2H), 7.53 (dt, $J = 19.6, 7.7$ Hz, 2H), 7.35 (dd, $J = 8.3, 4.5$ Hz, 2H), 7.27 (dt, $J = 17.1, 7.5$ Hz, 2H), 6.34 (d, $J = 8.4$ Hz, 2H), 6.27 (d, $J = 8.3$ Hz, 2H), 4.87 (dd, $J = 13.3, 5.8$ Hz, 1H), 3.63 (s, 3H), 3.05 (d, $J = 5.9$ Hz, 2H), 2.99 (s, 3H), 2.98 – 2.95 (m, 1H). ^{13}C NMR (150 MHz, CDCl_3) δ 171.10, 164.39, 154.42, 141.99, 137.40, 136.44, 136.11, 129.61, 129.19, 128.26, 125.61, 120.90, 120.28, 119.96, 114.5, 113.7, 108.9, 52.65, 51.34, 35.80, 30.91. Elemental analysis: calcd. C: 68.65, H: 5.01, N: 10.44, found: C:68.52, H:5.13, N:10.40.

Compound **19**. Yellow solid, yield of 50% (0.35g). MS-ESI, m/z 705 $[\text{M}+\text{H}]^+$. $[\alpha]_{\text{D}}^{25}$ -72.32 (c 2.95, CH_2Cl_2). **19A**: ^1H NMR (600 MHz, CDCl_3) δ 9.13 (s, 1H), 8.34 – 8.30 (m, 3H), 7.69 (q, $J = 7.2$ Hz, 2H), 7.53 (d, $J = 8.3$ Hz, 1H), 7.43 (t, $J = 7.5$ Hz, 2H), 4.97 (td, $J = 9.4, 4.4$ Hz, 1H), 3.73 (s, 4H), 3.48 (s, 4H), 1.76 (dd, $J = 11.5, 6.3$ Hz, 1H), 1.72 – 1.66 (m, 4H), 0.97 (t, $J = 5.4$ Hz, 6H), ^{13}C NMR (150 MHz, CDCl_3) δ 173.56, 165.11, 143.20, 138.49, 138.19, 137.41, 131.23, 129.34, 122.13, 121.49, 121.02, 115.03, 110.18, 52.26, 51.08, 41.67, 32.78, 25.15, 22.87, 22.00. **19B**: ^1H NMR (600 MHz, CDCl_3) δ 9.12 (s, 1H), 8.24 (d, $J = 8.5$ Hz, 1H), 7.69 (q, $J = 7.2$ Hz, 2H), 7.47 – 7.45 (m, 1H), 7.43 (t, $J = 7.5$ Hz, 2H), 4.86 (dd, $J = 8.7, 5.2$ Hz, 1H), 3.71 (s, 2H), 3.34 (s, 2H), 1.72 – 1.66 (m, 4H), 1.65 – 1.60 (m, 1H), 0.92 (d, $J = 6.2$ Hz, 2H), 0.88 (d, $J = 5.9$ Hz, 4H). ^{13}C NMR (150 MHz, CDCl_3) δ 173.08, 165.06, 143.02, 138.47, 137.92, 137.38, 131.09, 129.34, 121.99, 121.46, 120.99, 114.98, 109.84, 52.23, 50.69, 41.30, 32.31, 24.85, 22.85, 21.69. Elemental analysis for $\text{C}_{40}\text{H}_{44}\text{N}_6\text{O}_6$: calcd. C: 68.16, H: 6.29, N: 11.92, found: C:68.03, H:6.42, N:11.89.

Variable temperature ^1H NMR

Compound **13** (298 K, 25°C) **13A**: ^1H NMR (600 MHz, DMSO) δ 9.11 (s, H), 8.85 (d, $J = 8.1$ Hz, 1H), 8.59 (d, $J = 2.5$ Hz, 1H), 7.79 – 7.69 (m, 4H), 7.43 (td, $J = 7.2, 2.7$ Hz, 2H), 4.70 – 4.62 (m, 2H), 3.64 (s, 3H), 3.43 (s, 3H), 1.38 (d, $J = 7.2$ Hz, 3H). **13B**: ^1H NMR (600 MHz, DMSO) δ 9.12 (s, H), 8.88 (t, $J = 8.2$ Hz, 1H), 8.57 (d, $J = 2.5$ Hz, 1H), 7.79 – 7.69 (m, 4H), 7.43 (td, $J = 7.2, 2.7$ Hz, 2H), 4.70 – 4.62 (m, 2H), 3.61 (s, 3H), 3.35 (s, 3H), 1.40 (d, $J = 7.2$ Hz, 3H).

Compound **13** (323 K, 50°C) **13A**: ^1H NMR (600 MHz, DMSO) δ 9.10 (s, H), 8.75 (d, $J = 8.0$ Hz, 1H), 8.56 (s, 1H), 7.77 – 7.71 (m, 4H), 7.44 (dd, $J = 9.8, 4.9$ Hz, 2H), 4.67 (dt, $J = 14.8, 7.5$ Hz, 2H), 3.65 (s, 3H), 3.43 (s, 3H), 1.39 (d, $J = 7.2$ Hz, 3H). **13B**: ^1H NMR (600 MHz, DMSO) δ 9.10 (s, H), 8.78 (d, $J = 7.8$ Hz, 1H), 8.57 (s, 1H), 7.77 – 7.71 (m, 4H), 7.44 (dd, $J = 9.8, 4.9$ Hz, 2H), 4.67 (dt, $J = 14.8, 7.5$ Hz, 2H), 3.63 (s, 3H), 3.35 (s, 3H), 1.43 – 1.40 (m, 3H).

Compound **13** (353 K, 80°C), ^1H NMR (600 MHz, DMSO) δ 9.09 (s, 2H), 8.65 (s, 2H), 8.54 (s, 1H), 8.53 (s, 1H), 7.72 (s, 4H), 7.44 (dt, $J = 7.8, 3.8$ Hz, 2H), 4.68 (s, 2H), 3.65 (s, 6H), 3.43 (s, 3H), 3.36 (s, 3H), 1.42 (s, 6H).

Compound **13** (373 K, 100 °C), ^1H NMR (600 MHz, DMSO) δ 9.07 (s, 2H), 8.64 (s, 2H), 8.51 (s, 2H), 7.70 (s, 4H), 7.42 (s, 2H), 4.69 (s, 2H), 3.66 (s, 6H), 3.45 (s, 3H), 3.37 (s, 3H), 1.42 (s, 6H)

Compound **13** (393 K, 120 °C), ^1H NMR (600 MHz, DMSO) δ 9.08 (s, 2H), 8.63 (s, 2H), 8.50 (s, 2H), , 7.70 (s, 4H), 7.43 (s, 2H), 4.68 (s, 2H), 3.66 (s, 6H), 3.45 (s, 3H), 3.36 (s, 3H), 1.42 (s, 6H)

Computational methods

Conformational searches were performed firstly by using MMFF94S force field via two different packages, respectively. The stable conformations were 27 using Barista and 97 using Compute VOA, respectively. All the conformations were optimized at the B3LYP/6-31G(d) level in the gas phase. Total 21 conformations in 0-2.5 kcal/mol were selected for further optimizations

at the B3LYP/6-311+G(d) level and the B3LYP/6-311++G(2d,p) level in the gas phase and liquid, respectively. The geometries were then used for PES, TS computations and conformational analyses.

Acknowledgement

Authors thank the financial support from Hebei University for “Talent Program”, the Education Committee of Hebei Province (ZD2017004), and the computation support from the High-Performance Computer Center in Hebei University.

References and Notes

- (1) Zhu, H. J.; Jiang, J. X.; Saobo, S.; Pittman, C. U. *J. Org. Chem.* **2005**, *70*, 261–267.
- (2) (a) LaPlante, S. R.; Forgione, P.; Boucher, C.; Coulombe, R.; Gillard, J.; Hucke, O.; Jakalian, A.; Joly, M.; Kukolj, G.; Lemke, C.; McCollum, R.; Titolo, S.; Beaulieu, P. L.; Stammers, T. *J. Med. Chem.* **2014**, *57*, 1944–1951. (b) LaPlante, S. R.; Fader, L. D.; Fandrick, K. R.; Fandrick, D. R.; Hucke, O.; Kemper, R.; Miller, S. P. F.; Edwards, P. J. *J. Med. Chem.* **2011**, *54*, 7005–7022
- (3) (a) Ren, J.; Cai, X. H.; Fan, H. F.; Cao, J. X.; Liao, T. G.; Luo X. D.; Zhu, H. J. *Theochem.* **2008**, *870*, 72–76. (b) Bringmann, G.; Tasler, S. *Tetrahedron.* **2001**, *57*, 331–343
- (4) Modarresi-Alam, A. R.; Keykha, H.; Khamooshi, F.; Dabbagh, H. A. *Tetrahedron.* **2004**, *60*, 1525–1530.
- (5) (a) Gunter, H. *NMR spectroscopy*; 2nd ed. Wiley: New York, **1995**; Chapter 9. (b) Garratt, P. J.; Thom, S. N.; Wrigglesworth, R. *Tetrahedron.* **1994**, *50*, 12219–12234. (c) Carlson, E.; Jones, F. B.; Raban, M. *Chem. Commun.* **1969**, 1235–1237. (d) Dabbagh, H. A.; Modarresi-Alam, A. R. *J. Chem. Res. (S.)* **2000**, 190–192.
- (6) (a) Erol, S.; Dogan, I. *Chirality.* **2012**, *24*, 493–498. (b) Isikgor, F. H.; Erol, S.; Dogan, I.; *Tetrahedron: Asymmetry.* **2014**, *25*, 449–456. (c) Takahashi, I.; Morita, F.; Kusagaya, S.; Fukaya, H.; Kitagawa, O. *Tetrahedron: Asymmetry.* **2012**, *23*, 1657–1662. (d) Suzuki, Y.; Takahashi, I.; Dobashi, Y.; Hasegawa, H.; Roussel, C.; Kitagawa, O. *Tetrahedron Lett.* **2015**, *56*, 132–135. (e) Suzumura, N.; Kageyama, M.; Kamimura, D.; Inagaki, T.; Dobashi, Y.; Hasegawa, H.; Fukaya, H.; Kitagawa, O. *Tetrahedron Lett.* **2012**, *53*, 4332–4336.
- (7) Gasparri, F.; Lunazzi, L.; Mazzanti, A.; Pierini, M.; Pietrusiewicz, K. M.; Villani, C. *J. Am. Chem. Soc.* **2000**, *122*, 4776–4780.
- (8) Zhang, Y.; Wang, Y. Q.; Dai, W. M. *J. Org. Chem.* **2006**, *71*, 2445–2455.
- (9) (a) Yu, H.; Li, W. X.; Wang, J. C.; Yang, Q.; Wang, H. J.; Zhang, C. C.; Ding, S. S.; Li, Y.; Zhu, H. J. *Tetrahedron.* **2015**, *71*, 3491–3494. (b) Maurizio, P.; Fumio, S.; Hiroyuki, K.; Jun, U.; Shigeo, Y. *J. Org. Chem.* **1996**, *61*, 2122–2124.
- (10) Bai, B.; Shen, L.; Ren, J.; Zhu, H. J. *Adv. Synth. & Catal.* **2012**, *354*, 354–358.
- (11) Bai, B.; Zhu, H. J.; Pan, W. *Tetrahedron.* **2012**, *68*, 6829–6836.
- (12) Raban, M.; Jones, F. B. *J. Am. Chem. Soc.* **1971**, *93*, 2692–2699.
- (13) Frisch, M. J.; Trucks, G. W.; Schlegel, H. B.; Scuseria, G. E.; Robb, M. A.; Cheeseman, J. R.; Montgomery, J. A.; Vreven, Jr.; Kudin, T. K. N.; Burant, J. C.; Millam, J. M.; Iyengar, S. S.; Tomasi, J.; Barone, V.; Mennucci, B.; Cossi, M.; Scalmani, G.; Rega, N.; Petersson, G. A.;

Nakatsuji, H.; Hada, M.; Ehara, M.; Toyota, K.; Fukuda, R.; Hasegawa, J.; Ishida, M.; Nakajima, T.; Honda, Y.; Kitao, O.; Nakai, Klene, H. M.; Li, X.; Knox, J. E.; Hratchian, H. P.; Cross, J. B.; Adamo, C.; Jaramillo, J. R.; Gomperts, R. E.; Stratemann, O.; Yazyev, A. J.; Austin, R.; Cammi, C.; Ochterski, J. W.; Ayala, P. Y.; Morokuma, K.; Voth, G. A.; Salvador, P.; Dannenberg, J. J.; Zakrzewski, V. G.; Dapprich, S.; Daniels, A. D.; Strain, M. C.; Farkas, O.; Malick, D. K.; Rabuk, A. D.; Raghavachari, K.; Foresman, J. B.; Ortiz, J. V.; Cui, Q.; Baboul, A. G.; Clifford, S.; Cioslowski, J.; Stefanov, B. B.; Liu, G.; Liashenko, A.; Piskorz, P.; Komaromi, I.; Martin, R. L.; Fox, D. J.; Keith, T.; Al-Laham, M. A.; Peng, C. Y.; Nanayakkara, A.; Challacombe, M.; Gill, P. M. W.; Johnson, B.; Chen, W.; Wong, M. W.; Gonzalez, C.; Pople, J. A. *Gaussian 03 User's Reference*. Gaussian Inc. **2003**, Carnegie, PA.15106, USA.

(14) For TS calculations, see: (a) Zhu, H. J. *Organic Stereochemistry—experimental and computational methods*, Wiley-VCH, **2015**. (b) Zhu, H. J. *Modern Organic Stereochemistry*, Science Presses. (China), **2009**. (c) Xiao, W. L.; Lei, C.; Ren, J.; Liao, T. G.; Pu, J. X.; Pittman, C. U.; Lu, Y.; Zheng, Y. T.; Zhu, H. J.; Sun, H. D. *Chem.-A J. Eur.***2008**, *14*, 11584-11592. (d) Li, L. C.; Jiang, J. X.; Ren, J.; Ren, Y.; Pittman, C. U.; Zhu, H. J. *Eur. J. Org. Chem.* **2006**, 1981-1990.

(15) Foresman, J. B.; Frisch, A. E. *Exploring chemistry with electronic structure method*, 2nd ed. Gaussian, Inc. Pittsburg, PA. **1996**.

(16) (a) Berova, N.; Polavarapu, P. L.; Nakanishi, K.; Woody, R. W. *Comprehensive Chiroptical Spectroscopy*. John Wiley & Sons; Hoboken: New Jersey; **2011**. (b) Batista, J. M.; López SN, Jr.; Mota, J. S.; Vanzolini, K. L.; Cass, Q. B.; Rinaldo, D.; Vilegas, W.; Bolzani, V. S.; Kato, M.J.; Furlan, M. *Chirality* . **2009**, *21*, 799–801. (c) Stephens, P. J.; Pan, J. J.; Devlin, F. J.; Krohn, K.; Kurtan, T. *J Org Chem.***2007**, *72*, 3521-3536. (d) Zhu, H. J.; Li, W. X.; Hu, D. B.; Wen, M. L. *Tetrahedron.***2014**, *70*, 8236-8238. (e) Ren, J.; Li, G. L.; Shen, L.; Zhang, G. L.; Nafie, L.; Zhu, H. J. *Tetrahedron.* **2013**, *69*, 10351-10356. (f) Tirado-Rives, J.; Jorgensen, W. L. *J Chem Theo Comput* **2008**, *4*, 297-306. (g) Masullo, M.; Bassarello, C.; Bifulco, G.; Piacente, S. *Tetrahedron* .**2010**, *66*, 139–145. (h) Ding, Y. Q.; Li, X. C.; Ferreira, D. *J Nat Prod* .**2010**, *73*, 435–440. (i) He, P.; Wang, X. F.; Guo, X. J.; Zhou, C. Q.; Shen, S. G.; Hu, D. B.; Yang, X. L.; Luo, D. Q.; Rina, D.; Zhu, H. J. *Tetrahedron Lett* . **2014**, *55*, 2965–2968. (j) Zhao, S. D.; Shen, L; Luo, D. Q.; Zhu, H. J. *Cur Org Chem.* **2011**, *15*, 1843-1847. (k) Stephens, P; McCann, D. M.; Cheeseman, J. R.; Frisch, M. J. *Chirality.* **2005**, *17*, S52-S64. (l) Nakanishi, K.; Berova, N.; Woody, R. Ed.; VCH Publishers: New York, **1994**, 361-398.